Mosaic Models for Textures

NARENDRA AHUJA AND AZRIEL ROSENFELD, FELLOW, IEEE

Abstract—**This paper deals with a class of image models based on random geometric processes. Theoretical and empirical results on properties of patterns generated using these models are summarized. These properties can be used as aids in fitting the models to images.**

Index Terms—**Image models, mosaics, random geometry, texture.**

I. Introduction

TEXTURE perception is an important part of human vision [1]. Objects may often be distinguished by their characteristic textures in spite of similar colors or shapes. Textural cues are important in the perception of orientations and relative distances of surfaces [1]. The texture of a surface is characterized by properties such as fine, coarse, smooth, granulated, rippled, mottled, irregular, random, lineated, etc. [2].

Despite its ubiquity in scene analysis a precise definition of texture does not exist. Clearly, any such definition must be relatively simple and incorporate all important features of the texture that determine its various perceptual attributes. Pickett [1] views texture as consisting of a large number of elements, each in some degree visible, and, on the whole, densely and evenly (possibly randomly) arranged over the field of view such that there is a distinct characteristic spatial repetitiveness in the pattern.

All treatments of texture so far have taken one of the following two approaches.

The *statistical* approach [1], [3] attempts a global characterization of texture. Statistical properties of the spatial distribution of gray levels are used as texture descriptors. The key feature of this approach is the sole dependence of the description on point properties, with no explicit use of elements or subregions.

The *structural* approach conceives of texture as an arrangement of a set of spatial subpatterns according to certain placement rules [4]. The subpatterns themselves are, in general, made up of smaller subpatterns, positioned according to some placement rules. This recursive nature of the approach captures the hierarchical structure of natural scenes. Both the subpatterns and their placement may be characterized statistically.

Most existing texture models are based upon the first approach. While statistical models may be successfully used in discriminating sets of textures, and in other such limited tasks, it is our contention that they are inherently less powerful than the structural models that use probabilistic subpattern selection and placement. For the case of images on grids this is not hard to see. Consider a subpattern that consists of a single pixel. It is obvious that its characteristics and placement rules can be designed so as to make the resulting model identical to any given statistical model, since both have control over the same set of image primitives and can incorporate the same types of primitive interactions. This shows that the structural models are at least as powerful as the statistical models. On the other hand, it is obvious that images that are piecewise uniform with respect to some property, and are known to have been generated by a structural approach, must be better modeled using the structural approach. Similar arguments apply to Euclidean plane textures. However, it is not clear if the lower power of the statistical approaches really makes them less useful for image modeling, since limitations of human visual perception may make the additional power of the structural approach unexploitable, and hence, insignificant.

Natural phenomena involve objects of variable physical extent. At any resolution, therefore, natural textures are likely to consist of more than one pixel. However, it is not obvious what the structure should be. At times, a good guess about the physical processes that may have given rise to a given pattern may provide clues as to the appropriate structure a model must incorporate. Pattern generation processes in nature are certainly very complex, and usually impossible to simulate exactly. However, it may be useful to single out some important features of these processes. If a model can incorporate such features, the patterns it describes may be similar to real textures in significant ways.

As we will see in Section II, little effort has been devoted to the structural approach. Even for the few structural models that have been considered, there has not been a reasonable amalgamation of the various properties we have discussed above. These methods either are not generative or involve training based upon some arbitrarily selected features, or are not well analyzed as regards their properties.

In this paper we describe a class of generative models called mosaic models that use random pattern generation processes in the plane to provide image structure.

In Section II we review the models of texture that have been proposed earlier, including both statistical and structural models.

Section III describes two classes of mosaic models, called cell structure and coverage ("bombing") models, and gives several examples of each. The general treatment of mosaic models in the rest of the paper uses these examples as illustrations. As

Manuscript received April 2, 1979; revised January 8, 1980. This work was supported by the U.S. Air Force Office of Scientific Research under Grant AFOSR-77-3271.

N. Ahuja was with the Computer Science Center, University of Maryland, College Park, MD 20742. He is now with the Coordinated Science Laboratory and the Department of Electrical Engineering, University of Illinois, Urbana, IL 61801.

A. Rosenfeld is with the Computer Science Center, University of Maryland, College Park, MD 20742.

0162-8828/81/0100-0001$00.75

we will note in Section VII, a variety of models could be added to the small set used here. We also discuss some aspects of the grid version of the mosaics originally defined in the Euclidean plane. We conclude the section by outlining a methodology for obtaining a model for a given image.

Some of the geometrical features proposed in Section III are obtained for the cell structure models in Section IV. We derive expressions for the expected area of a connected component, expected width of a component, expected number of components, and expected total perimeter in the image, for the three regular and three random cell structure models that constitute our repertoire of such models. We also obtain the same set of geometrical properties for the square and circular coverage models, for both the binary and multicolored cases.

In Section V we discuss properties of the mosaic models that represent the correlation between the pixels in terms of their relative positions. We derive the joint gray level probability density of pixels at a given distance and orientation for the two classes of models. These density functions are then used to obtain the autocorrelation function, the edge density, and the variogram for the models. The relationship between the responses of some digital edge operators and the Euclidean plane perimeter is also discussed.

Section VI briefly discusses the problem of fitting mosaic models to real textures, and presents some preliminary results. Section VII summarizes the work presented in this paper. It critically reviews the mosaic model approach in comparison with the other methods. Some projects that could be undertaken to further investigate the application of mosaic models are suggested.

II. Texture Models

This section reviews texture models under the statistical and structural classes. See [14] for an alternate classification.

A. Statistical Models

The models based upon the statistical approach can be divided into two major classes: time series models and random field models.

1) Time Series Models: Time series analysis [5] has been extensively used to study visual textures. In the simplest form, the image is TV scanned to provide a one-dimensional series of gray level fluctuations, which is treated as a one-dimensional stochastic process evolving in "time." Alternatively, a point is assumed to depend upon a certain part of its neighborhood and on Gaussian noise. The coefficients of dependence are extracted from the images by using time series analysis techniques. Various forms of the dependence provide different models.

By studying the statistical properties of a given texture, e.g., its autocorrelation function, etc., McCormick and Jayaramamurthy [6] have made a choice of a best fitting time series model for a given texture. They also use the same information to estimate the required set of parameter values, and generate synthetic textures using the model.

In an earlier paper Whittle [7] pointed out the difficulty of using time series for two-dimensional processes. The problem is that in a two-dimensional process, the dependence of a point extends in all directions, and there is no direct way to map the two-dimensional grid points onto a series such that the original dependence is preserved, although it is unilateral (depends only on the past values). In view of this, one would like to try to capture as much of the two-dimensional dependence as possible without getting into the analytical problems due to bilateral dependence. Tou *et al.* [8] have done this by making a point depend on its upper and left neighbors. They consider fitting a model to a given texture. The choice among the various models, as well as the choice of the order of the process, is made by comparing the behavior of some observed statistical properties, e.g., the autocorrelation function, with that predicted by each of the different models. For each of the possibly many choices of models, the values of the parameters are determined so as to minimize, say, the least-square error in fit. In a subsequent paper, Tou and Chang [9] use the maximum likelihood principle to optimize the values of the parameters, in order to obtain a refinement of the preliminary model as suggested by the autocorrelation function.

2) Random Field Models: The second class of models treats the image as a two-dimensional random field (for a definition of random field, see Wong [10]).

One way to describe a random field would be in terms of the joint probability density of the properties (say, gray level) of the pixels, although this may be an overspecification, i.e., the modeling may not represent enough abstraction. It also implies estimation of the spatial probability density functions of gray levels, which means inference on the joint probability density of a large number of random variables corresponding to the pixels in the entire image. One immediate simplification that could be introduced is to assume that not all points in an image are simultaneously constrained by a high-dimensional probability density function, but that this is only true of small neighborhoods of pixels. However, even for a neighborhood of size 3×3 (or 5×5) and nonparametric representation one has to deal with densities in a 9- (or 25-) dimensional space, along with the associated sample size and storage problems. This makes the approach unwieldy.

Read and Jayaramamurthy [11] and McCormick and Jayaramamurthy [12] make use of switching theory techniques to identify textures by describing their local gray level patterns using minimal functions. If each pixel can take one out of N_g gray levels, then a given neighborhood of n pixels from an image can be represented by a point in an $(n \times N_g)$-dimensional space. If many such neighborhoods from a given texture are considered then they are likely to provide a cluster of points in the above space. The differences in the local characteristics of different textures are expected to result in different clusters. The set covering theory of Michalski and McCormick [13], which is a generalization of the minimization machinery of switching theory already available, is used [12] to describe the sets of points in each cluster. These maximal descriptions also allow coverage of empty spaces

within and around clusters, and thus the samples do not have to be exhaustive but only have to be large enough to provide a good representation of the underlying texture.

Haralick *et al.* [14] confine the local descriptions to 2×1 neighborhoods. They identify a texture by the gray level cooccurrence frequencies at neighboring pixels, which are the first estimates of the corresponding probabilities. They use several different features, all derived from the cooccurrence matrix, for texture classification.

Deguchi and Morishita [15] use a noncausal model for the dependence of a pixel on its neighborhood centered at the pixel. The weights are determined by minimizing the mean-square estimation error. The optimal two-dimensional estimator characterizes the texture. They use such a characterization for classification and for segmentation of images consisting of more than one textural region.

In view of the seemingly difficult task of describing or extracting the joint probability densities, attempts have been made to use parametric models where the form of the probability density is assumed, or to model the field density by specifying some "important" properties of the field that may correspond to more than one probability density function.

Among parametric models of the joint density of pixels in a window, the multivariate normal has been the one most commonly used because of its tractability. However, it has been found to have limited applicability [16]. Hunt [17], [18] points out that stationary, Gaussian modeling of images is an oversimplification. He proposes a nonstationary Gaussian model which differs from the stationary model only in that the mean vector has unequal components. He shows the appropriateness of this model by subtracting, from each point on the image, its local ensemble average, and showing that the resulting picture fits a stationary Gaussian model.

Trussel and Kruger [19] show that the Laplacian density function constitutes a more valid model for high-pass filtered imagery than the Gaussian model. They show that this discrepancy neither seriously weakens the applicability of this class of models to a major restoration method nor challenges any other conclusions of the work based on the Gaussian model.

Longuet-Higgins [20]-[22] treats the ocean surface as a random field satisfying the following assumptions:

a) the wave spectrum contains a single, narrow band of frequencies; and

b) the wave energy is being received from a large number of different sources whose phases are random.

Some of the results that he derives are:

1) the probability distribution of the surface elevation, and that of the magnitude and orientation of the gradient;

2) the average number of zero crossings per unit distance along a line in an arbitrary direction;

3) the average length of contour per unit area;

4) the average density of maxima and minima per unit area; and

5) for a narrow spectrum, the probability distribution of the heights of maxima and minima.

All the results are expressed in terms of the two-dimensional energy spectrum up to a finite order only. The converse of the problem is also studied and solved, i.e., given certain statistical properties of the surface, to find a convergent sequence of approximations to the energy spectrum.

The analogy between this work and image processing, and the significance of the results obtained therein, is obvious. Fortunately, the assumptions made are also acceptable for images.

Panda [23] uses an analogous approach to analyze background regions selected from forward-looking infrared (FLIR) imagery. He derives expressions for 1) density of border points and 2) average number of connected components in a row of the thresholded picture. There is good agreement between the observed and the predicted values in most cases, for most of the pictures considered. Panda [24] also uses the same model to predict the properties of the pictures obtained by running several edge operators (based on differences of average gray levels) on some synthetic pictures with normally distributed gray levels, and having different correlation coefficients. The images are assumed to be continuous-valued stationary Gaussian random fields with continuous parameters.

Matheron [25] uses the change in pixel properties as a function of distance to model a random field. He uses the term regionalized variables to emphasize the particular features of the pixels whose complex mutual correlation reflects the structure of the underlying phenomenon. He assumes weak stationarity of the increments in the gray levels between pixels. The second moment of the increments for pixels at an arbitrary distance, called the variogram, is used to reflect the structure of the field. Knowledge of the variogram is useful for the estimates of many global and local properties of the field. Huijbregts [26] discusses several properties of the variogram and relates them to the structural features of the regionalized variables. For nonhomogeneous fields having spatially varying mean, the variogram of the residuals with respect to the local means is used.

A characterization similar to the variogram is given by the autocorrelation function. In work on image restoration, images have often been modeled by a two-dimensional random field with a given mean and autocorrelation. An autocorrelation function that has been found to be reasonably good for a variety of pictorial data is

$$R(\tau_1, \tau_2) = \sigma^2 \exp\left[-\alpha_1 |\tau_1| - \alpha_2 |\tau_2|\right],$$

which is stationary and separable.

Nahi and Jahanshahi [27] suggest modeling the image as a background statistical process combined with a set of foreground statistical processes, each replacing the background in the regions occupied by the objects of the category which it is assumed to characterize.

In a subsequent paper Nahi and Lopez-Mora [28] use a more complex γ function. For each row, γ either indicates the absence of the object or provides a vector estimate of the object width and its geometric center in that row. The two-dimensional vector possesses information about the object

size and skewness, and is assumed to be a first-order Markov process.

Abend *et al.* [16] introduce Markov Meshes to model dependence of a pixel on a certain immediate neighborhood. The joint probability density for the entire image, then, is the product of local conditional probability densities at each pixel. Using Markov chain methods on the sequences of pixels from various causal dependency neighborhoods of a pixel they show that in many cases such a causal dependence translates into a noncausal dependence. For example, the dependence of a pixel on its west, northwest and north neighbors translates into its dependence upon all its eight neighbors. Interestingly, the causal neighborhood that results in a 4-neighbor noncausal dependence is not known.

Hassner and Sklansky [29] also discuss a Markov random field model for images. They present an algorithm that generates a texture from an initial random configuration and a set of independent parameters that specify a consistent collection of nearest neighbor conditional probabilities which characterize the Markov random field.

Pratt and Faugeras [30] and Gagalowicz [31] view texture as the output of a homogeneous spatial filter excited by white noise, not necessarily Gaussian. The image is then characterized by its mean, the histogram of the input white noise, and the transfer function of the filter. For a given texture, the model parameters are obtained as follows.

- The mean is readily estimated from the image.
- Computing the autocorrelation function (second-order moments) determines the magnitude of the transfer function.
- Computing higher order moments determines the phase of the transfer function.

Inverse filtering gives the white noise image and hence its histogram and probability density. For a Markov field of order 1 it may be sufficient to replace the decorrelation operator by a Laplacian, or by gradient operators. However, the whitened field estimate of the independent identically distributed noise process obtained above will only identify the spatial operator in terms of the autocorrelation function, which is not unique. Thus, the white noise probability density and the spatial filter do not, in general, make up a complete set of descriptors [32]. But it may be possible that they are sufficient descriptors from the standpoint of visual texture discrimination.

Mandelbrot also takes a similar approach although he views the pixel gray levels as defining a Brownian surface [33].

B. Structural Models

The next three models use the notion of a structural primitive, although both the shapes of the primitives and the rules to generate the textures from the primitives may be specified statistically. This statistical-structural nature of these models brings them closer to the models discussed in the following sections than any of the models described so far.

Matheron [34] and Serra [35] propose a model that views a binary texture as produced by a set of translations of a structural element. All locations of the structural elements such that the entire element lies within the foreground of the texture are identified. Note that there may be (narrow) regions which cannot be covered by any placement of the structural element, as all possible arrangements of the element that cover a given region may not lie completely within the foreground. Thus, only an "eroded" version of the image can be spanned by the structural element which is used as the representation of the original image. Textural properties can be obtained by appropriately parameterizing the structure element. It is interesting to note that for a structural element consisting of two pixels at distance d, the area of the eroded image is the value of the autocovariance, at distance d, of the original image. More complicated structural elements would provide a generalized autocovariance function which has more structural information. Matheron and Serra show how the generalized covariance function can be used to obtain various texture features.

Zucker [36] conceives of a real texture as being a distortion of an ideal texture which is a spatial layout of primitives as cells in a regular or semiregular tessellation. Certain transformations are applied to the primitives to distort them to provide a realistic texture. The statistical nature of the texture can be provided through these transformation rules.

Yokoyama and Haralick [37] describe a growth process to synthesize textures. Their method consists of the following steps.

1) Mark some of the pixels in a clean image as seeds.
2) The seeds grow into curves called skeletons.
3) The skeletons thicken to become regions.
4) The pixels in the regions thus obtained are transformed into gray levels in the desired range.
5) A probabilistic transformation is applied, if desired, to modify the gray level cooccurrence probability in the final image.

The distribution processes in step 1) and the growth processes in steps 2) and 3) can be deterministic or random. The dependence of the properties of the images generated on the nature of the underlying operations is not obtained. This makes the approach unsuitable for texture description or classification.

There are a number of other studies of texture that are more technique oriented, and describe some ad hoc texture feature selection and classification schemes which are not based upon any specific model of the texture. We are concerned here with models of texture and hence will not discuss these studies; see [2] for a good survey.

III. Mosaic Models

This section briefly reviews some planar geometrical processes that define the proposed class of models. A more detailed treatment of this material can be found in [38].

A. Cell Structure Models

Cell structure mosaics are constructed in two steps.

1) Tessellate a planar region into cells. We will only consider tessellations composed of bounded convex polygons.

2) Independently assign one of m colors to each cell according to a fixed set of probabilities

$$p_1, \cdots, p_m; \quad \sum_{i=1}^{m} p_i = 1.$$

The set of colors may correspond to a set of values of any property, not necessarily gray level.

Cell structure models form a family whose members differ in the manner in which the plane is tessellated. We will describe some important members of this family, starting from the three regular tessellations and progressing towards random ones.

1) Checkerboard Model: In this model, the origin and orientation of the axes are chosen randomly, and the plane is tessellated into squares.

2) Hexagonal Model: This is analogous to the checkerboard model, except that the plane is tessellated into regular hexagons.

3) Triangular Model: This is analogous to the first two models, but based on a tessellation into equilateral triangles.

4) Poisson Line Model: In this model, a Poisson process chooses points in the strip $0 \leqslant \theta < \pi$, $-\infty < \rho < \infty$. Each of these points defines a line of the form $x \cos\theta + y \sin\theta = \rho$, and these lines define a tessellation of the plane.

5) Occupancy Model: In this model, a Poisson process chooses points (called "nuclei") in the plane. Each nucleus defines a "Dirichlet cell" consisting of all the points in the plane that are nearer to it than to any other nucleus.

6) Delaunay Model: The Delaunay tessellation is obtained by joining all pairs of nuclei whose Dirichlet cells are adjacent.

B. Coverage Models

Coverage or "bombing" models constitute the second class of mosaic models that we consider. A coverage mosaic is obtained by a random arrangement of a set of geometric figures ("bombs") in the plane.

We will first describe the process defining the class of binary models. Consider the geometric figure in the plane and identify it by 1) the location of some distinguished point in the figure, e.g., its center of gravity, hereafter called the center of the figure; and 2) the orientation of some distinguished line in the figure, e.g., its principal axis of inertia. Let a point process drop points on the plane and let each point represent the center of a figure. Let each figure have an orientation θ according to some distribution function $F(\theta)$. By this process any fixed region A is randomly partitioned into A_0 and $A_1 = A - A_0$, where A_1 consists of that part of A that is covered by the figures. By assigning two different colors to A_0 and A_1, we get a binary coverage mosaic.

A multicolored coverage mosaic is obtained by considering figures of more than one color. The color of a given figure is randomly chosen from a known vector of colors $\bar{c} = (c_1, c_2, \cdots, c_m)$ according to a predetermined probability vector $\bar{p} = (p_1, p_2, \cdots, p_m)$. Let c_0 denote the background color. Since the figures, in general, overlap, we must have a rule to determine the colors of the regions that are covered by figures of more than one color. We will give one example of such a rule. Let us view the point process as dropping the centers sequentially in time. Each time a new point falls, the area covered by the associated figure is colored with the color of that figure irrespective of whether any part of the area has already been included in any of the previously fallen figures. The color of a point in the final pattern is thus determined by the color of the latest figure that covered it. (Note that we could just as well have allowed a figure to cover only an area not included in any of the previous figures.)

More generally, we can have more than one type of geometric figure, with the sizes of each class of figures governed by a certain probability distribution. These along with the nature of the point process and the choices of the probability distributions for color and orientation selection provide different ways of controlling the characteristics of the resulting patterns.

The coverage models discussed in this paper use a Poisson point process for dropping centers, and figures of a fixed shape and size. Some examples of the figures that can be considered are line segments, ellipses, circles, rectangles, and squares.

C. Digital Mosaics

All the models described above use processes that are defined in the Euclidean plane. On a grid these processes can at best be simulated only coarsely. Often, many of the concepts of the Euclidean plane must be almost completely redefined in order to be adaptable to a grid. Moreover, even with the modified definitions, the digital plane patterns are not as well behaved as the Euclidean plane patterns. Many measures become meaningless for extreme values of the quantities they describe. As a general rule, digital versions of Euclidean plane phenomena become better and better behaved with increasing resolution, i.e., with a finer and finer grid. Therefore, we can expect digital mosaics to behave only approximately as they would in the Euclidean plane, and we should preferably work at high resolution.

During the course of the work described in this paper we have faced several problems originating from the discrete nature of the grid. We have had to modify several Euclidean plane definitions to suit the grid patterns. To illustrate this, we briefly discuss the Poisson process on the grid.

In the Euclidean plane, a point process is said to be a homogeneous Poisson point process of intensity λ if:

1) the number of points in any region of area A has a Poisson distribution with parameter λA; and

2) the numbers of points in disjoint regions are independent random variables.

Any finite region in the Euclidean plane is mapped onto a finite number of points on the grid, so that whereas the actual Poisson process can drop an unlimited number of points with positive probability in such a region, the digital Poisson process can drop at most as many points as there are grid points in the region. Since each grid point represents a square of unit area centered at that point in the plane, it will be selected by the digital Poisson process whenever even a single point is dropped by the Euclidean Poisson process in the square. From property 1) above, we have

$p \equiv$ Pr {a given point on the grid is occupied by the digital Poisson process of intensity λ}

= Pr {a square of unit area in the Euclidean plane contains at least one point due to a Poisson process of intensity λ}

$= 1 - e^{-\lambda}$.

A digital Poisson point process is thus a binomial process with parameter $p = 1 - e^{-\lambda}$, and

Pr {n points fall in a region consisting of N grid points}

$$= \binom{N}{n} p^n (1-p)^{N-n}.$$

To simulate a Poisson process on the grid thus amounts to making a binary decision at each of its points.

D. Analysis of Models

In applying models such as those discussed above to images, we should use properties of the models that can be directly measured for a given image, so that we can determine the degree of the fit of the model to the image. Some examples of such properties are as follows.

1) What is the probability that a pair of points distance d apart will fall in regions of colors c_i and c_j? In other words, for each d, what is the color cooccurrence matrix?

2) What is the expected number of connected components of color c_i?

3) What is the expected area of a connected component of color c_i? Or, what is the total area having color c_i? Note that in the case of cell structure models this information is implicit in the answer to question 2) above, since from the model we already know the stationary probability vector of the colors. This is because the cells are nonoverlapping. However, in the case of coverage models this question involves a different property.

4) What is the nature of the autocorrelation function?

5) What is the expected perimeter density? Alternatively, what is the edge density?

6) What is the expected squared color difference (variogram) for point pairs?

In the following sections we present results regarding these properties for the models discussed above.

IV. Geometric Properties of Components

A connected component of uniformly colored points in a mosaic will be called a component of the mosaic. These components are unions of identically colored, adjacent units (cells or figures). Geometrical properties of components are important because, in analyzing an image, we cannot isolate single units.

In this section we discuss geometrical properties of components in both cell structure and coverage mosaics, including the expected area and width of a component, the expected number of components, and the expected total component perimeter in the mosaic. Only a brief summary of the results is given here; the details can be found in two papers [39], [40].

A. Cell Structure Mosaics

Let us first consider an $M \times N$ checkerboard mosaic in which the squares have two possible colors, black and white, with the probability of a black square being p, and that of a white square being $q = 1 - p$. Let $E(r)$ be the expected number of runs (of black squares) of length r in a row; readily we have $E(N) = p^N$, while $E(r) = (N - r - 1)p^r q^2 + 2p^r q$ for $0 < r < N$. Moreover, the total expected number of runs in a row is $(N - 1)qp + p$. Let $T(r)$ be the expected number of distinct components reaching a given row whose runs in that row are overlapped by a run of length r in the next row; we have estimated $T(r)$ empirically. Then the increment in the number of components when a row is added is given by

$$\sum_{r=1}^{N} E(r)[q^r + (1 - q^r)(1 - T(r))].$$

The expected number of components in the mosaic is then

$$C = C_0 + (M-1)\Delta = \frac{\sum_{r=1}^{N} E(r) + (M-1)\Delta}{M} + (M-1)\Delta$$

where C_0 is the expected number of components in the first row.

The expected number of black squares in the mosaic is $B = pMN$; hence the expected number of squares in a component is $A = B/C$. It is not hard to show that the expected perimeter in a component (i.e., the expected number of pairs of adjacent black and white squares such that the black square belongs to the component) is $P = 4Aq$, since $4q$ is the expected number of white neighbors of a black square.

We can carry out an analogous analysis for a hexagonal mosaic, by treating it as a checkerboard in which alternate rows have been shifted by half the square size. Here we use increments Δ_o and Δ_e corresponding to the addition of odd- and even-numbered rows, respectively. We then have

$$C = C_0 + \left\lceil \frac{M-1}{2} \right\rceil \Delta_e + \left\lfloor \frac{M-1}{2} \right\rfloor \Delta_o.$$

The expected number of black cells is $B = p(\lfloor M/2 \rfloor \lceil N/2 \rceil + \lceil M/2 \rceil \lfloor N/2 \rfloor)$, and the expected number of hexagons in a component is thus $A = B/C$. Similarly, the expected number of white neighbors of a black cell is $6q$, and P is thus $6Aq$.

The analysis for a triangular mosaic is also analogous, except that here we have $B = pMN$ (as in the checkerboard case), and the expected number of white neighbors of a black cell is $3q$.

Let us now consider any regular tessellation in which each cell has K neighbors (sharing an edge with it), and V cells meet at each vertex. Evidently, for the square, hexagonal, and triangular tessellations we have $K = 4, 6, 3$, and $V = 4, 3, 6$, respectively. It is easily seen that the results obtained above apply to any mosaics having the same K and V values.

Finally, consider a random tessellation in which the expected number of neighbors of each cell is K, and the expected number of cells meeting at a vertex is V. We conjecture that in the random mosaic defined by any such tessellation, the expected values for the number, area, and perimeter of

TABLE I
PREDICTED AND OBSERVED NUMBERS OF BLACK COMPONENTS IN A 100-CELL RANDOM MOSAIC

Black cell probability (p)	Poisson line mosaic		Occupancy mosaic		Delaunay mosaic	
	Predicted	Observed	Predicted	Observed	Predicted	Observed
.1	8.0	8.0	8.6	7.0	8.2	10.7
.2	14.2	14.7	11.8	10.7	14.4	15.7
.3	14.5	13.7	11.7	9.3	17.1	17.3
.4	12.1	10.0	10.2	10.0	19.3	15.3
.5	8.9	9.0	7.2	5.0	16.4	17.3
.6	6.2	4.7	4.1	3.7	11.9	9.0
.7	3.1	2.3	2.7	2.3	9.7	6.0
.8	1.6	2.3	2.0	1.7	4.3	3.3
.9	1.0	1.3	2.0	1.0	1.7	1.0

black components are the same as those for a regular mosaic with the same K and V values. Now it is known [38] that the expected K and V values for the Poisson line, occupancy, and Delaunay tessellations are the same as the K and V values for the regular square, hexagonal, and triangular tessellations, respectively. Also the area and perimeter properties of the individual cells of these tessellations are known [38]. Hence our conjecture enables us to predict the expected number, area, and perimeter of black components in the cell structure models.

The predictions and observed values for the expected numbers C of components in random mosaics having 100 cells are summarized in Table I as functions of the black cell probability p. We see that the agreement is generally good, especially when p is small. This analysis readily extends to mosaics with more than two colors, since we can group all but one of the colors together to obtain the two-color case.

Finally, we consider the expected width W of a component, i.e., the expected run length of points of a given color along a line drawn across the mosaic. Let p_i be the probability that a cell has the given color. For a checkerboard mosaic of square side b, we can show that

$$W = \frac{\sqrt{2}b}{\pi(1 - p_i)} \ln \frac{\sqrt{2} + 1}{\sqrt{2} - 1}.$$

Similarly, for a triangular mosaic we have

$$W = \frac{3\sqrt{3}b}{4\pi(1 - p_i)} \ln 3.$$

The expression for the hexagonal mosaic is more complicated and will not be given here.

For the random mosaics, we can use the fact that the mean chord length of a convex region of area A and perimeter P is $\pi A/P$. Applying this to the cells of the mosaics, we have

$$W = \frac{\pi}{1 - p_i} E(A/P)$$

where $E(\ )$ means "the expected value of." For a Poisson line model in which the Poisson process has intensity τ/π, we have $E(A) = \pi/\tau^2$ and $E(P) = 2\pi/\tau$. For an occupancy or Delaunay model in which the process has intensity λ, we similarly have $E(A) = 1/\lambda$, $E(P) = 4/\sqrt{\lambda}$ and $E(A) = 1/2\lambda$, $E(P) = 32/3\pi\sqrt{\lambda}$, respectively. We can use these values, together with the approximation $E(A/P) = E(A)/E(P)$ [39], to estimate W for these mosaics.

B. Coverage Mosaics

Our approach to estimating the expected number of connected components in a coverage mosaic is also based on analysis of runs of overlapping components; for an $M \times N$ digital image it has the form

$$C = C_0 + (M - 1)\,\Delta$$

just as in Section IV-A. Now the expected image area occupied by the figures is

$$A_c = MN(1 - e^{-\lambda\alpha})$$

where λ is the intensity of the Poisson process and α is the area of each figure. Thus the expected area of a component is A_c/C. Explicit expressions for C_0 and Δ can be given in the cases of square and circular figures.

The estimation of expected perimeter for coverage mosaics depends on determining, for each figure, the total length of its border segments that are not intersected by any other figure. An exact formula can be given for the expected perimeter in Euclidean plane mosaics. However, for the grid case we have obtained only an approximate expression.

For square figures, Table II shows expected and predicted number of components, covered area, and perimeter for a 200×200 image. These quantities are tabulated as functions of the expected number n of square centers per square area. (This parameter n takes into account both the intensity λ of the Poisson process and the area a of the squares.) The agreement appears to be quite good.

We can also consider the expected component width W in coverage mosaics; the details will not be given here. These results all assume a two-color mosaic (figures and background); the generalization to multicolor mosaics is quite complicated (except for the expected perimeter and covered area), and has not been attempted.

V. CORRELATION PROPERTIES OF MOSAICS

This section discusses properties involving the gray levels of pairs of points in an image generated by a mosaic model. We discuss the joint gray level probability density for pairs of

TABLE II
PREDICTED AND OBSERVED NUMBERS OF COMPONENTS, COVERED AREAS, AND PERIMETERS FOR A SQUARE COVERAGE MOSAIC

Square centers per square area	Number of components		Covered area		Perimeter	
	Predicted	Observed	Predicted	Observed	Predicted	Observed
.1	125.6	129.2	3806.5	3939.4	3183.8	3421.6
.5	200.7	205.6	15738.8	15408.0	8189.2	9108.6
1.0	38.8	38.0	25284.8	25286.0	7858.0	9150.6
1.5	4.3	3.0	31074.8	31065.8	5986.6	6798.8
2.0			34586.6	34688.8	4206.3	4569.4
2.5			36716.6	36630.4	2843.0	3052.0
3.0			38008.5	37934.0	1880.1	1942.0
4.0			39267.4	34276.2	792.9	702.8

points at given separations, and also derive from it the autocorrelation, edge density, and variogram (expected squared gray level difference) for the mosaics. Only a brief summary of results is given here; the details can be found in [41].

A. Joint Gray Level Probability

For the cell structure models, let $W(d)$ be the probability that two points distance d apart lie in the same cell. Explicit expressions for $W(d)$ can be given for the square, hexagonal, and triangular tessellations; for example, for squares of side b we have

$$W(d) = \begin{cases} 1 - (4d/\pi b) + (d^2/\pi b^2) & d \leqslant b \\ 1 - (2/\pi) - (4/\pi)\cos^{-1}(b/d) - (d^2/\pi b^2) \\ \quad + (4/\pi)\sqrt{(d^2/b^2) - 1} & b < d \leqslant \sqrt{2}b \\ 0 & d > \sqrt{2}b. \end{cases}$$

For the Poisson line model with intensity τ/π we have $W(d) = e^{-2\tau d/\pi}$. Explicit expressions for $W(d)$ for the occupancy and Delaunay models are not known, but we have empirically estimated these functions.

In terms of $W(d)$, the probability density $P_{ij}(d)$ for one of a randomly selected pair of points at distance d having color c_i, given that the other point has color c_j, is given by

$$P_{ij}(d) \equiv p_i p_j (1 - W(d)) + \delta_{ij} W(d)$$

where δ_{ij} is the Kronecker delta.

For the coverage models, the analysis depends on the probabilities that figure centers do or do not occur in specified areas centered at the two points. For any area A, no centers occur in A with probability $e^{-\lambda A}$, and at least one center occurs with probability $1 - e^{-\lambda A}$, where λ is the intensity of the Poisson process. For a two-color model the probabilities are of the form

$$P_{\text{white, white}}(d, \theta) = e^{-\lambda(2A_1 - A_2(d,\theta))}/p_{\text{white}}$$
$$P_{\text{white, black}}(d, \theta) = 2e^{-\lambda A_1}[1 - e^{-\lambda(A_1 - A_2(d,\theta))}]/p_{\text{black}}$$
$$P_{\text{black, white}}(d, \theta) = -2e^{\lambda A_1}[1 - e^{-\lambda(A_1 - A_2(d,\theta))}]/p_{\text{white}}$$
$$P_{\text{black, black}}(d, \theta) = \{1 - e^{-\lambda A_1}[2 - e^{-\lambda(A_1 - A_2(d,\theta))}]\}/p_{\text{black}}.$$

The areas themselves have relatively complicated expressions determined by the geometry of the figures. For example, for upright black squares of side length $2a + 1$ on a white background, we have

$$A_1 = 4a^2$$

and

$$A_2(d, \theta) = 4a^2 - 2ad(\sin\theta + \cos\theta) + (d^2/2)\sin 2\theta$$
$$\text{for } 0 \leqslant d \leqslant 2a$$
$$\text{or } \cos^{-1}(2a/d) \leqslant \theta \leqslant \pi/4$$
$$= 0 \quad \text{otherwise.}$$

The expressions for multicolored models are more complicated.

B. Autocorrelation

For a cell structure model the covariance $\text{cov}(d)$ of two points distance d apart having gray levels x and y is $E(xy) - E(x)E(y)$, where $E(xy) = W(d)E(x^2) + (1 - W(d))E^2(x)$, so that $\text{cov}(d) = W(d)[E(x^2) - E^2(x)]$. Hence, the autocorrelation coefficient $\rho(d)$ is $\text{cov}(d)/\text{cov}(0) = W(d)$. It is interesting to note that for the Poisson line model $W(d)$ is negative exponential, a commonly assumed form for the autocorrelation of an image; but for the other cell structure models, this is not the case.

For a two-color coverage model it can be shown that

$$\rho(d, \theta) = \frac{e^{-\lambda A_1}}{1 - e^{-\lambda A_1}}[e^{\lambda A_2(d,\theta)} - 1]$$

where A_1 and A_2 are as in Section V-A. Expressions for autocorrelation for the multicolored models can also be obtained.

C. Edge Density

Let P be the expected border length per unit area in a continuous mosaic as discussed earlier. Since in all our models the border consists of randomly oriented straight line segments, it is not very hard to see that the expected number of horizontal and vertical steps in the chain code of the digital border is $4P/\pi$, and the expected number of diagonal steps is

$$4P(\sqrt{2} - 1)/\pi.$$

Let δ denote the expected absolute difference between two different colors; then the expected (e.g., horizontal) edge value per unit area is $2P\delta/\pi$. Analogous expressions can be obtained for other edge operators.

D. Variogram

The variogram of an image is the expected squared difference between the gray levels of two randomly selected points at a given separation. For the cell structure models we have

$$\gamma(d) = (1 - W(d)) \sum_{i,j=1}^{m} (c_i - c_j)^2 p_i p_j.$$

For two-color coverage models we have

$$\gamma(d, \theta) = 2e^{-\lambda A_1} [1 - e^{-\lambda(A_1 - A_2(d,\theta))}] (B - W)^2$$

where B and W are the two colors, and A_1, A_2 are as in Section V-A. The corresponding expression for multicolored coverage models can also be obtained.

VI. Fitting Mosaic Models to Textures

In [42] some preliminary experiments on fitting mosaic models to real textures were described. Predicted variograms were computed for two models, checkerboard and Poisson line, and were fitted to the actual variograms of ten texture samples from Brodatz' album. These textures were also thresholded, and average component widths were computed for them. This width agreed very closely with the width predicted by the better fitting model in each case.

Some further experiments on mosaic model fitting are reported in [43]. Samples of four Brodatz textures and three terrain textures were segmented, and average component area and perimeter and total number of components were computed. Values predicted by six cell structure models (checkerboard, hexagonal, triangular, Poisson line, occupancy, and Delaunay) were also computed. (Predictions were also made for the square bombing model, but they were very poor in all cases.) For each texture, the model parameters were adjusted to make the area predictions match the observed values, and the resulting errors in predicted perimeter were tabulated; and vice versa. The minimum area error and minimum perimeter error models for each texture were the same in nearly all cases, and were consistent from sample to sample for nearly all the textures.

VII. Concluding Remarks

The following are some specific points of comparison between mosaic models and conventional statistical texture models, such as time series and random field models.

1) Mosaic models describe images by specifying geometrical processes that may have generated the visual pattern under consideration. Such a constructive description, therefore, inherently encompasses the specification of all the information about the pattern. One may extract from the model as much information as desired, e.g., autocorrelation properties, which may not be unique to the image. For example, characterization of a pattern in terms of its autocorrelation properties ignores any phase information.

It may be interesting to note that certain features of some of the mosaic models are the same as have been commonly used to model images. At the same time, other mosaic models take different values for the same features, thus implying that mosaic models should prove to be a more general class of models. As an example, the Poisson line model has an exponential autocorrelation function, a model that has been extensively used in the literature; while other mosaic models exhibit different forms of autocorrelations.

2) Time series models allow the current value of an image point to depend on a finite number of previous values. There is, thus, an inherent assumption in the definition of the model about the Markovianity of the data. While it is a different issue how useful the model could still be in practice, such an assumption places a definite theoretical restriction on the generality of the model. Both the random field and mosaic models are free of such a restriction.

3) Images are inherently two-dimensional and hence should be treated as such. Time series models clearly fail to meet this requirement. They allow a point to depend on, at best, only a part of its neighborhood. A time series model also cannot make use of the rich class of two-dimensional features, e.g., shape and orientation of subpatterns, edge density, connectedness of components, etc., which seem to play an important role in human perception of images. Some of these features have one-dimensional counterparts which could, in principle, be used. But they are much less useful because of their lesser semantic relevance. The random field and mosaic models, on the other hand, are two-dimensional models.

4) In time series modeling the choice of the model is based upon a qualitative assessment of the autocorrelation function. The order of the underlying process is guessed, to begin with, and then iteratively improved until a set of parameter values is found that, along with the chosen order of the model, predicts an autocorrelation function sufficiently close to the observed one. Thus, the process of model specification involves some amount of trial and error.

For random field models there is a much larger gap between the variety of models proposed and the attempts at fitting them to images. Except for some simple parametric models, however, the model fitting does appear to be a complex process.

Furthermore, the model arrived at in order to obtain a good fit of properties such as autocorrelation may, in fact, turn out to be worse than expected, due to the fact that the characterization of the image in terms of correlation properties ignores phase information, as pointed out in 1) above.

It may be observed that in both the time series and random field models the complexity of modeling is very unevenly shared by the two levels of a) model selection and b) parameter evaluation. There is only a limited choice about the type of model to be selected, and the parameterization of the chosen model is the major part of the modeling process. The variety of natural images must, therefore, be represented only by the assignment of distinct values to the parameter set of the model.

Mosaic models, on the other hand, are much richer in variety, and each of these models is simpler to specify, as compared to

the time series and random field models. The complete process of modeling thus gets more evenly split into the two steps. This should have the effect of reducing the size of the search space when fitting models to a given image.

5) Natural visual patterns can often be characterized by a repetitive arrangement of certain subpatterns, according to a set of rules. The subpatterns, recursively, may be patterns of smaller extent, but of independent complexity (busyness, entropy, fineness). A small set of relatively less busy subpatterns with sharp borders may give the image a patchy appearance, whereas a large set of busy patterns may give rise to a finer, textured pattern.

One reason why mosaic models may be more appropriate for complex natural images is that they provide a hierarchical character to the problem of image modeling. The arrangement of the components, possibly of more than one type, in the mosaic is often specified statistically.

For the nonpatchy class of patterns, both the time series and random field models may not turn out to be very complex. Although one could also attempt to apply these models to images with regularly shaped patches having relatively sharp borders, such an approach is likely to defy an easy analysis, and is likely to provide a complex model. For example, the order of the resultant time series model may be very high in order to incorporate enough information about the gray level jumps across the patch borders. Clearly, although the interior patch-points do not contain much information, they do increase the order of the model, making it more complex and computationally more expensive.

Not surprisingly, in view of the above observations, the time series models have been used only for those images that are relatively well suited for such an approach, as pointed out above. The images used for most of the random field models that have been tried also are relatively nonpatchy.

It may be seen that an image from the patchy category can be transformed into a picture of the nonpatchy category by sampling it sufficiently coarsely. Since this transformation should not change the structure of the image, the model should still be valid with a different set of parameter values. The validity of the choice of a mosaic model thus appears to be insensitive to scale changes, and mimics the underlying generating process of the image so as to incorporate as much of the detail as is captured in the image to be modeled.

Under certain conditions the mosaic models and the random field models may produce similar patterns. For example, a random field model may fit certain coarsely sampled (dense) mosaics.

6) Mosaic models are likely to be intuitively more meaningful. A pattern corresponding to a specified model, and the implications for it of the variations in parameter values, may be easier to visualize in case of the mosaic models than the others.

In conclusion, mosaic models provide a powerful set of tools for texture analysis and synthesis. The large number of possible models provides a means of controlling or matching many different texture features. It is planned to undertake a series of studies in which these models are applied to the analysis of real textures.

Acknowledgment

The authors express their thanks to E. Slud for many helpful discussions and to K. Riley for her help in preparing this paper.

References

[1] R. M. Pickett, "Visual analysis of texture in the detection and recognition of objects," in *Picture Processing and Psychopictorics*, B. S. Lipkin and A. Rosenfeld, Eds. New York: Academic, 1970, pp. 289-308.

[2] R. M. Haralick, "Statistical and structural approaches to texture," in *Proc. 4th Int. Joint Conf. Pattern Recognition*, Nov. 1978, pp. 45-69.

[3] J. K. Hawkins, "Textural properties for pattern recognition," in *Picture Processing and Psychopictorics*, B. S. Lipkin and A. Rosenfeld, Eds. New York: Academic, 1970, pp. 347-370.

[4] A. Rosenfeld and B. S. Lipkin, "Texture synthesis," in *Picture Processing and Psychopictorics*, B. S. Lipkin and A. Rosenfeld, Eds. New York: Academic, 1970, pp. 309-322.

[5] J. E. P. Box and G. M. Jenkins, *Time Series Analysis.* San Francisco, CA: Holden-Day, 1976.

[6] B. H. McCormick and S. N. Jayaramamurthy, "Time series model for texture synthesis," *Int. J. Comput. Inform. Sci.*, vol. 3, pp. 329-343, 1974.

[7] P. Whittle, "On stationary processes in the plane," *Biometrika*, vol. 41, pp. 434-449, 1954.

[8] J. T. Tou and Y. S. Chang, "An approach to texture pattern analysis and recognition," in *Proc. 1976 IEEE Conf. Decision Contr.*, Dec. 1976, pp. 398-403.

[9] J. T. Tou, D. B. Kao, and Y. S. Chang, "Pictorial texture analysis and synthesis," in *Proc. 3rd Int. Joint Conf. Pattern Recognition*, Nov. 1976.

[10] E. Wong, "Two-dimensional random fields and representations of images," *SIAM J. Appl. Math.*, vol. 16, pp. 756-770, 1968.

[11] J. S. Read and S. N. Jayaramamurthy, "Automatic generation of texture feature detectors," *IEEE Trans. Comput.*, vol. C-21, pp. 803-812, 1972.

[12] B. H. McCormick and S. N. Jayaramamurthy, "A decision theory method for the analysis of texture," *Int. J. Comput. Inform. Sci.*, vol. 4, pp. 1-38, 1975.

[13] R. S. Michalski and B. H. McCormick, "Interval generalization of switching theory," in *Proc. 3rd Annu. Houston Conf. Comput. Syst. Sci.*, Houston, TX, Apr. 1971, pp. 213-226.

[14] R. M. Haralick, K. Shanmugam, and I. Dinstein, "Textural features for image classification," *IEEE Trans. Syst., Man, Cybern.*, vol. SMC-3, pp. 610-621, 1973.

[15] K. Deguchi and I. Morishita, "Texture characterization and texture-based image partitioning using two-dimensional linear estimation techniques," *IEEE Trans. Comput.*, vol. C-27, pp. 846-850, 1978.

[16] K. Abend, T. J. Harley, and L. N. Kanal, "Classification of binary random patterns," *IEEE Trans. Inform. Theory*, vol. IT-11, pp. 538-544, 1965.

[17] B. R. Hunt, "Bayesian methods in nonlinear digital image restoration," *IEEE Trans. Comput.*, vol. C-26, pp. 219-229, 1977.

[18] B. R. Hunt and T. M. Cannon, "Nonstationary assumptions for Gaussian models of images," *IEEE Trans. Syst., Man, Cybern.*, vol. SMC-6, pp. 876-882, 1976.

[19] H. J. Trussel and R. P. Kruger, "Comments on nonstationary assumptions for Gaussian models in images," *IEEE Trans. Syst., Man, Cybern.*, vol. SMC-8, pp. 579-582, 1978.

[20] M. S. Longuet-Higgins, "The statistical analysis of a random moving surface," *Phil. Trans. Roy. Soc. London*, vol. A249, pp. 321-387, Feb. 1957.

[21] —, "Statistical properties of an isotropic random surface," *Phil. Trans. Roy. Soc. London*, vol. A250, pp. 151-171, Oct. 1957.

[22] —, "On the statistical distribution of the heights of sea waves," *J. Marine Res.*, vol. 11, pp. 245-266, 1952.

[23] D. P. Panda, "Statistical properties of thesholded images," *Comput. Graphics Image Processing*, vol. 18, pp. 334-354, 1978.

[24] D. P. Panda and T. Dubitzki, "Statistical analysis of some edge operators," *Comput. Graphics Image Processing*, vol. 11, pp. 313-348, 1979.

[25] G. Matheron, "The theory of regionalized variables and its applications," *Les Cahiers du Centre de Morphologie Math. de Fontainbleau*, vol. 5, 1971.

[26] C. Huijbregts, "Regionalized variables and quantitative analysis of spatial data," in *Display and Analysis of Spatial Data*, J. Davis and M. McCullagh, Eds. New York: Wiley, 1975, pp. 38–51.
[27] N. E. Nahi and M. H. Jahanshahi, "Image boundary estimation," *IEEE Trans. Comput.*, vol. C-26, pp. 772–781, 1977.
[28] N. E. Nahi and S. Lopez-Mora, "Estimation detection of object boundaries in noisy images," *IEEE Trans. Automat. Contr.*, vol. AC-23, pp. 834–845, 1978.
[29] M. Hassner and J. Sklansky, "Markov random field models of digitized image texture," in *Proc. 4th Int. Joint Conf. Pattern Recognition*, Nov. 1978, pp. 538–540.
[30] W. K. Pratt and O. D. Faugeras, "Development and evaluation of stochastic-based visual texture features," in *Proc. 4th Int. Joint Conf. Pattern Recognition*, Nov. 1978, pp. 545–548.
[31] A. Gagalowicz, "Analysis of texture using a stochastic model," in *Proc. 4th Int. Joint Conf. Pattern Recognition*, Nov. 1978, pp. 541–544.
[32] W. K. Pratt, O. D. Faugeras, and A. Gagalowicz, "Visual discrimination of stochastic texture fields," *IEEE Trans. Syst., Man, Cybern.*, vol. SMC-8, pp. 796–804, 1978.
[33] B. Mandelbrot, *Fractals–Form, Chance, and Dimension.* San Francisco, CA: Freeman, 1977.
[34] G. Matheron, *Elements pour une Theorie des Milieux Poreux.* Paris: Masson, 1967.
[35] J. Serra and G. Verchery, "Mathematical morphology applied to fibre composite materials," *Film Sci. Technol.*, vol. 6, pp. 141–158, 1973.
[36] S. Zucker, "Toward a model of texture," *Comput. Graphics Image Processing*, vol. 5, pp. 190–202, 1976.
[37] R. Yokoyama and R. M. Haralick, "Texture synthesis using a growth model," *Comput. Graphics Image Processing*, vol. 8, pp. 369–381, 1978.
[38] B. Schachter and N. Ahuja, "Random pattern generation processes," *Comput. Graphics Image Processing*, vol. 10, pp. 95–114, 1979.
[39] N. Ahuja, "Mosaic models for images, 1: Geometric properties of components in cell structure mosaics," *Inform. Sci.* to be published.
[40] —, "Mosaic models for images, 2: Geometric properties of components in coverage mosaics," *Inform. Sci.* to be published.
[41] —, "Mosaic models for images, 3: Spatial correlation in mosaics," *Inform. Sci.* to be published.
[42] B. J. Schachter, A. Rosenfeld, and L. S. Davis, "Random mosaic models for textures," *IEEE Trans. Syst., Man, Cybern.*, vol. SMC-8, pp. 694–702, 1978.
[43] N. Ahuja and A. Rosenfeld, "Fitting mosaic models to textures," in *Image Texture Analysis*, R. M. Haralick, Ed. New York: Plenum, 1981.
[44] —, "Image models," in *Handbook of Statistics*, P. R. Krishnarah and L. N. Kanal, Eds., to be published.

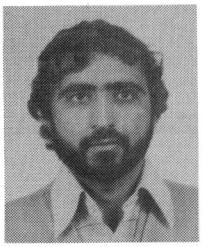

Narendra Ahuja was born in Achnera, India, on December 8, 1950. He received the B.E. degree with honors in electronics engineering from the Birla Institute of Technology and Science, Pilani, India, in 1972, the M.E. degree with distinction in electrical communication engineering from the Indian Institute of Science, Bangalore, India, in 1974, and the Ph.D. degree in computer science from the University of Maryland, College Park, in 1979.

From 1974 to 1975 he was Scientific Officer in the Department of Electronics, Government of India, New Delhi. From 1975 to 1979 he was at the Computer Vision Laboratory, University of Maryland, College Park, as a Graduate Research Assistant (1975–1978), as a Faculty Research Assistant (1978–1979), and as a Research Associate (1979). In 1979 he joined the University of Illinois, Urbana-Champaign, where he is currently a Research Assistant Professor in the Coordinated Science Laboratory and an Assistant Professor in the Department of Electrical Engineering. His research interests are in computer vision and pattern recognition.

Dr. Ahuja is included in *Who's Who in Technology Today*, and is a member of the Association for Computing Machinery, the IEEE Computer Society, and Sigma Xi.

Azriel Rosenfeld (M'60–F'72) was born in New York, NY, on February 19, 1931. He received the B.A. degree in physics from Yeshiva University, New York, NY, and the Ph.D. degree in mathematics from Columbia University, New York, NY, in 1950 and 1957, respectively.

From 1954 to 1956, he was a Physicist with the Fairchild Controls Corporation, New York, NY; from 1956 to 1959, he was an Engineer with the Ford Instrument Company, Long Island City, NY; and from 1959 to 1964, he was Manager of Research with the Budd Company Electronics Division, Long Island City, NY, and Information Sciences Center, McLean, VA. Since 1964, he has been a Professor of Computer Science at the University of Maryland, College Park. He has published ten books and nearly 250 papers, most of them dealing with the computer analysis of pictorial information. He edits the journal *Computer Graphics and Image Processing* and was Chairman of the Third International Joint Conference on Pattern Recognition.